# CHAPTER 7

# SIMULATION OF FOAM IMPACT EFFECTS ON COMPONENTS OF THE SPACE SHUTTLE THERMAL PROTECTION SYSTEM

**Eric P. Fahrenthold**[1] **and Young-Keun Park**[2]

Department of Mechanical Engineering, 1 University Station C2200
University of Texas, Austin, TX 78712, USA

[1]Professor, corresponding author, phone: (512) 471-3064, email: epfahren@mail.utexas.edu
[2]Graduate student

## ABSTRACT

A series of three dimensional simulations has been performed to investigate analytically the effect of insulating foam impacts on ceramic tile and reinforced carbon-carbon components of the Space Shuttle thermal protection system. The simulations employed a hybrid particle-finite element method and a parallel code developed for use in spacecraft design applications. The conclusions suggested by the numerical study are in general consistent with experiment. The results emphasize the need for additional material testing work on the dynamic mechanical response of thermal protection system materials, and additional impact experiments for use in validating computational models of impact effects.


## NOMENCLATURE

| | |
|---|---|
| $\mathbf{c}$ | particle center of mass position vector |
| $d$ | element shear damage variable |
| $D$ | element normal damage variable |
| $\mathbf{E}^p$ | element plastic strain tensor |
| $\mathbf{f}$ | particle damping force |
| $m$ | particle mass |
| $\mathbf{p}$ | particle translational momentum vector |
| $S$ | particle entropy |
| $V$ | thermomechanical potential energy function |

## INTRODUCTION

The report of the Columbia Accident Investigation Board[1] concluded that the effects of foam impact on the wing leading edge of the Space Shuttle was the most likely cause for the loss of the Orbiter Columbia. Strong evidence in support of this conclusion is provided by a recent series of impact experiments conducted at Southwest Research Institute (SwRI) by a NASA-SwRI-industry team.[2] The current consensus regarding the cause of the accident was not present in the early stages of the investigation, since little experimental data relevant to the accident conditions was available, and since significant lead times were required to prepare and conduct the necessary impact experiments.

Soon after the loss of Columbia an impact analysis team was assembled[3] whose purpose was to investigate analytically the effects of foam impact on components of the Space Shuttle thermal protection system, and to support the conduct of experiments designed to duplicate the impact events observed during launch of the vehicle. This group included NASA, industry, national laboratory, and university participation and employed a variety of numerical methods[4] and computer codes[5] to simulate the impact events of interest. The present paper describes simulations performed using a hybrid particle-finite element method[6] and a parallel computer code[7] to model the impact of foam blocks on both ceramic tile and reinforced carbon-carbon (RCC) components of the Space Shuttle thermal protection system. The simulations described here were performed in advance of the aforementioned experiments and employed the best available material property data for foam, tile, and RCC. The conclusions suggested by the simulations are in general consistent with the results of later experiments, although additional material testing, material modeling, and simulation work is needed to develop a validated computational approach to impact damage assessment for future Space Shuttle applications.

The sections which follow describe the numerical method used in the simulations, the structural and material models assumed for the foam projectiles and the ceramic tile or RCC targets, the computational costs of the simulations, and the results of the numerical study, including suggestions for future research.

## NUMERICAL METHOD

In recent research focused on the design of orbital debris shielding, a new numerical method and parallel computer code have been developed for use in spacecraft design applications. This hybrid numerical method employs in tandem nondeforming Lagrangian particles and large strain finite element kinematics,[8] to simulate impact problems involving shock loading, large deformation plasticity, and complex fragmentation dynamics. The method has been implemented in a three dimensional code and validated by comparison with published experiments at impact velocities ranging from one to eleven kilometers per second.[9]

The hybrid method combines the general contact-impact modeling capabilities of particle methods with a true Lagrangian description of strength effects, the latter offered by finite element techniques. It avoids

the tensile instability problems which have hindered the effective use of some particle techniques, as well as the mass and energy discard normally associated with Lagrangian finite element models of material failure. No particle to element mapping is required, since both particles and elements are used throughout the calculation, but to represent distinct physical effects. The particles model all inertia and all contact-impact as well as volumetric thermomechanical response in compressed states, while the elements model tension and elastic-plastic shear. Material failure is represented by the loss of element cohesion, after which particles not associated with any intact element are free to flow under general contact-impact loads.

In the case of spherical particles, the state space model for the particle-element system[8] consists of evolution equations for the particle translational momenta ($\mathbf{p}^{(i)}$) and center of mass position vectors ($\mathbf{c}^{(i)}$)

$$\dot{\mathbf{p}}^{(i)} = -\frac{\partial V}{\partial \mathbf{c}^{(i)}} - \mathbf{f}^{(i)} \,, \qquad \dot{\mathbf{c}}^{(i)} = m^{(i)-1}\, \mathbf{p}^{(i)} \tag{1}$$

augmented by evolution equations for the internal state variables

$$\dot{S}^{(i)} = \dot{S}^{(i)}(\mathbf{p}^{(i)}, \mathbf{c}^{(i)}, S^{(i)}, d^{(j)}, D^{(j)}, \mathbf{E}^{p(j)}) \tag{2}$$

$$\dot{d}^{(j)} = \dot{d}^{(j)}(\mathbf{p}^{(i)}, \mathbf{c}^{(i)}, S^{(i)}, d^{(j)}, D^{(j)}, \mathbf{E}^{p(j)}) \tag{3}$$

$$\dot{D}^{(j)} = \dot{D}^{(j)}(\mathbf{p}^{(i)}, \mathbf{c}^{(i)}, S^{(i)}, d^{(j)}, D^{(j)}, \mathbf{E}^{p(j)}) \tag{4}$$

$$\dot{\mathbf{E}}^{p(j)} = \dot{\mathbf{E}}^{p(j)}(\mathbf{p}^{(i)}, \mathbf{c}^{(i)}, S^{(i)}, d^{(j)}, D^{(j)}, \mathbf{E}^{p(j)}) \tag{5}$$

where $\mathbf{f}^{(i)}$ is a damping force, $m^{(i)}$ is a particle mass, $S^{(i)}$ is a particle entropy, $d^{(j)}$ and $D^{(j)}$ are element shear and normal damage variables, $\mathbf{E}^{p(j)}$ is a plastic strain tensor, $i$ is a particle index, $j$ is an element index, and $V$ is a thermomechanical potential

$$V = V(\mathbf{c}^{(i)}, S^{(i)}, d^{(j)}, D^{(j)}, \mathbf{E}^{p(j)}) \tag{6}$$

The specific functional forms of the thermomechanical potential and the internal state evolution equations depend upon the constitutive assumptions as well as the adopted interpolations for the density and displacement fields. The present work investigated for the first time the application of this method to a relatively low velocity impact regime, in problems which nonetheless involved complex contact-impact, material failure, and fragmentation phenomena difficult to simulate using structural finite element codes.

## MATERIAL MODELS

The simulations described here employed simple material models for the foam, tile, felt strain isolation pad (SIP), and RCC, with material properties estimated using the available experimental data. All materials were assumed to be isotropic elastic-perfectly plastic,[10] with an accumulated a plastic strain criterion applied to initiate element failure. The available material data base may be summarized as follows. In support of the Columbia accident investigation, Glenn Research Center[11] and Sandia National Laboratories (SNL)[12] performed mechanical property tests on foam, tile, and reinforced carbon-carbon. Mechanical property tests previously performed on SIP and on SIP-tile combinations are described by Sawyer[13] and Cooper and Sawyer[14] respectively. The relevant thermal properties for polyurethane, tile, SIP, and carbon-carbon materials are provided by Oertel,[15] Banas et al.,[16] Myers et al.,[17] Ohlhorst et al.,[18] and the commercial literature.[19]

Table 1 lists estimated properties for the materials of interest. These values were used (except in the case of the SIP) to perform the simulations described in this paper. The present analysis adopted a yield strength for the tile corresponding to the lowest experimental measurements of Lu et al.[12] In the case of the RCC, the present analysis assumed a yield strength equal to the bending strength measured by Lu et al.,[12] since the failure mode for the RCC panels was expected to be flexure of the panel surface under the foam impact load. At the time the present analysis was performed, the data available to the authors on SIP properties was very limited. As a result the SIP density was underestimated by a factor of 2.3, and the single layer of SIP elements used in the numerical model was assigned the same stiffness properties as the tile. The effect of the underestimating the SIP density was to slightly underestimate the target areal density, and in the present analysis is not considered to be significant. The experiments of Cooper and Sawyer[14] suggest that the stiff SIP elements used here would tend to overestimate the tile damage produced by the foam impact load.

More general models of the dynamic mechanical deformation and failure of the foam, tile, felt, and reinforced carbon-carbon materials are needed. The authors and others are currently engaged in work to develop improved material models, with anisotropy and strain rate dependence significant in some if not all

of these materials.

## TILE IMPACT MODEL

Analysis of launch videos, supplemented by computational fluid dynamics studies, suggested that ceramic tiles located on the lower surface of Columbia might have been struck by a block of insulating foam shed from the vehicle's external tank. A series of experiments was therefore planned to measure the impact damage produced by highly oblique foam block impacts on tile arrays similar to those covering the lower surface of the Orbiter wing. Simulations were run in advance of these experiments, to estimate the impact damage. The simulation parameters are listed in Table 2.

In each simulation the target model was composed of a 2 x 4 foot array of tiles, each tile having an areal extent of 6 x 6 inches. The uniform tile thickness matched that in the suspected impact areas, over the main landing gear door and in the nearby wing acreage. In the simulations the tile array was supported by an aluminum plate, whose lower surface was fixed along a circumferential edge strip, the latter with a width of one inch. The strain isolation pad (SIP) which separates the tile and the aluminum wing structure was modeled with a single layer of finite elements, however similar (gap filler) material often interposed between the individual tiles was not modeled. The foam projectile was modeled as a homogeneous hexahedral block. The dimensions, obliquity, and orientation of the foam block at impact were varied between simulations, due to uncertainties in the interpretation of the launch videos, a dependence of the impact obliquity on the vehicle impact location, and a desire to investigate the effect of projectile orientation (roll angle) on impact damage.

Computer resource requirements and some limitations of the research code and preprocessor used here made it necessary to introduce certain geometric approximations. Since available commercial preprocessors do not generate hybrid particle-finite element models, a special preprocessor was employed. The latter code generates solid models composed of uniform hexahedra, and associated ellipsoidal particles, so that an element and particle deletion process was used to introduce the gaps between the tiles. As a result the width of these gaps was overestimated. Combined with the aforementioned neglect of gap fillers, the assumed geometric

model approximates conservatively the structural strength of the actual tile array. A second approximation was introduced in modeling the individual tiles, whose external surfaces are coated in a borosilicate layer, to a depth approximately five percent of the tile thickness. Computer resource requirements precluded modeling of features with such small dimensions, so the tiles were taken to be monolithic with material properties derived from the published strength and stiffness properties of an individual tile.

## TILE IMPACT SIMULATIONS

The four tile impact simulations were performed on systems operated by NASA Ames Research Center, and required between three and five wall clock days on 128 or 192 processors of an SGI Origin. The models were composed of over one million particles, with the simulations extending over five or six milliseconds of physical time.

The first two simulations differed only with respect to projectile orientation (roll angle), and modeled the impact of a 1.06 pound block of foam, at a velocity of 700 feet per second, on a tile array similar to those which cover the main landing gear doors. Impact obliquity was five degrees. The simulations showed 12.0 cubic inches of material (0.178 tile volumes) eroded by the long edge impact and 19.6 cubic inches of material (0.290 tile volumes) eroded by the short edge impact. Figures 1 and 2 show the simulation results, including views of the predicted tile erosion. In both these simulations the maximum predicted depth of penetration was approximately one half of the tile thickness. Since the short edge impact appeared to be more damaging under the postulated impact conditions, subsequent simulations (and later experiments) involved foam blocks rotated so as to strike the tile array along the projectile's short edge. Experiments which approximately correspond to these two simulations were later performed by Kerr et al.[2] The first experiment produced three craters with a total volume of approximately 0.1 cubic inches, although much of this damage may have been caused by the unintended impact of a Mylar burst disc used in the compressed air gun which launched the projectile. The second experiment produced no impact craters. Since the aforementioned numerical modeling assumptions minimized both tile strength and tile lateral support while maximizing the stiffness of the SIP layer, the tile impact damage was overestimated. However the eroded volume error was less than

one third of one tile volume, with the damage distributed among several tiles.

The third and fourth simulations considered somewhat more severe impact conditions. The third case assumed a 2.24 pound projectile and a slightly reduced tile thickness (tile thickness varies with position over the lower surface of the Orbiter). The result was an increase in eroded material, to 48.2 cubic inches (0.789 tile volumes) and an increase in the maximum depth of penetration, to three quarters of the tile thickness. These simulation results are depicted in Figure 3. Finally the fourth case considered a lower mass projectile (1.53 pounds), but a slightly higher impact velocity (720 fps) and a more direct impact, with the impact obliquity taken to be thirteen degrees. The tile thickness in the target was increased in order to represent a wing acreage area away from the main landing gear door. The simulation results, shown in Figure 4, predicted erosion of 70.6 cubic inches of material (0.785 tile volumes) and a maximum depth of penetration to the level of the SIP, in one small area. Experiments which approximately correspond to these two simulations were later performed by Kerr et al.[2] The first experiment produced no impact craters. The second experiment produced four craters, each with an areal extent of less than 1.0 square inches (depth not provided). It appears that the aforementioned numerical modeling assumptions again caused the tile impact damage to be overestimated. The eroded volume error was less than one tile volume, with the damage distributed among multiple tiles.

In summary the pretest simulations predicted in the worst case the removal of less than one tile volume of ceramic material, under modeling assumptions which conservatively approximated tile strength properties, the lateral support provided in the tile gap region, and the compliance of the SIP layer. Subsequent testing showed that none of the impact configurations considered here produced significant damage to the target tile array.

## RCC IMPACT MODEL

As in the case of the underwing tiles, analysis of launch videos and complimentary computational fluid dynamics work suggested the possibility that Columbia's wing leading edge was subjected to a highly oblique foam block impact. A series of experiments on reinforced carbon-carbon panels was therefore planned to

investigate the effects of such impacts, for panel geometries representative of the leading edge region most likely involved. Prior to these experiments, two simulations were run to estimate the impact damage. The simulation parameters are listed in Table 3.

The target model used in the simulations represented the geometry of wing leading edge panel number six. The limitations of the preprocessor used here again led to certain approximations. A profile for the model cross section was obtained by fitting coordinate data extracted from a CAD model of the actual panel, and assuming a constant RCC wall thickness. This cross section was then extended an axial distance equal to the total panel length, with stiffening ribs added at both ends, similar to those found on the actual part. The upper and lower edges of the panel were held fixed in the simulations. This target model was considered to be generally representative of the strength and stiffness of the actual structure. The simulations assumed that in the RCC elements failure would occur at a plastic strain of 0.01, a relatively brittle failure criterion. The thin silicon carbide coating present on the actual part was not modeled, again due to the high computational cost of simulations which resolve very small scale features. As discussed in a preceding section, the particle-element preprocessor used here produced models composed of uniform hexahedra, so that the curved surface of the RCC panel model was represented with a stairstep geometry.

The starting conditions for the two simulations differed only with respect to projectile orientation (roll angle), one objective of the analysis being to determine the relative severity of impact damage caused by edge and corner impacts. The specified impact point was located a distance of 18.1 inches from the panel edge, measured along the panel arc, and the impact obliquity (14.6 degrees) was specified as the angle between the target surface normal at the impact point and the projectile velocity vector, the latter aligned with the long axis of the foam block. The pitch, roll, and yaw of the projectile were computed so as to match these specifications.

## RCC IMPACT SIMULATIONS

The RCC panel impact simulations were performed on SGI Origin systems at NASA Ames Research Center, and required between three and four wall clock days on 128 or 256 processors. The models were

composed of approximately two million particles, with the simulations extending over no more than two milliseconds of physical time. The simulation results are depicted in Figure 5 (corner impact case) and Figure 6 (edge impact case). The first simulation modeled a corner impact and resulted in failure of the panel, with a crack approximately six inches in length developing along the panel surface, normal to the leading edge stagnation line. The second simulation modeled an edge impact and showed greater panel damage, in this case multiple cracks, the largest extending along half the length of the panel and aligned parallel to the stagnation line.

Although the scope of the RCC impact simulation work described here was limited, the results indicate failure of the panel under the postulated foam impact loads. These results are in general consistent with later experiments conducted on Space Shuttle wing leading edge panels. Experiments which approximately correspond to these two simulations were performed by Kerr et al.[2] In the first experiment, a corner impact test conducted on a panel six target at a twenty-one degree obliquity resulted in a crack of length 5.5 inches located at the panel edge and oriented parallel to the stagnation line. In the second experiment, an edge impact test conducted on a panel eight target at a twenty-five degree obliquity resulted in gross failure of the panel surface, producing a 17 inch by 16 inch hole in the panel surface. Comparison of the experiments and simulations is complicated by differences in target geometry and impact obliquity. Since the experiments involved higher impact obliquities, they would be expected to produce more damage than is depicted in the simulations. The first simulation showed a crack similar in size to that observed in the first experiment, although the predicted location and orientation were not correct. The second simulation showed large cracks in the panel surface, at an impact obliquity ten degrees less than that which resulted in gross panel failure in the second experiment. In general the numerical modeling work, which incorporated best case assumptions with regard to RCC strength and ductility, appears to provide good estimates of panel impact damage.

## CONCLUSION

The present paper has described a series of pre-test simulations performed to estimate damage produced by external foam strikes on thermal protection system components of the Space Shuttle. The simulations

employed a hybrid particle-finite element technique and a parallel computer code developed for use in spacecraft design applications. The simulation results are in general consistent with experimental results available for this class of problems, and indicate that the numerical method used here is suitable for application in a relatively low velocity regime. The application of this numerical technique to future impact problems would be facilitated by further methods and interface development work, aimed at accommodating complex structural geometries described by a standard CAD data base or a commercial finite element preprocessor.

Several conclusions specific to the operation of the Space Shuttle and the design of future aerospace planes are suggested: (1) additional material testing and constitutive modeling research describing the deformation and failure of thermal protection system materials is needed, (2) numerical methods and code development work is needed to provide a validated computer simulation capability for impact damage assessment, (3) additional, higher resolution simulations should be performed, to investigate the effects of any simplifying assumptions made in the areas of material modeling and structural geometry, and (4) additional impact testing should be conducted, over a wider range of impact conditions, to validate proposed computational analysis techniques.

Research in the suggested areas is already in progress. The authors are currently engaged in work which will allow the hybrid particle-finite element technique used here to model impact on any structural geometry described by a general hexahedral finite element mesh.

*Acknowledgments* — This work was supported by the Space Science Branch of NASA Johnson Space Center (NAG 9-1244) and by the National Science Foundation (CMS 99-12475). Computer time support was provided by the NASA Advanced Supercomputing Division of Ames Research Center and by the Texas Advanced Computing Center at the University of Texas at Austin.

## REFERENCES

1. Report of the Columbia Accident Investigation Board, Volume 1, Government Prining Office, Washington, DC, August 2003.

2. J.H. Kerr, D.J. Grosch, and E.L. Christiansen, "Impact Testing of Large Foam Projectiles," AIAA-2004-0939, presented at the 2004 AIAA Aerospace Sciences Meeting, Reno, Nevada, January 5-8,2004.

3. R.F. Stellingwerf, J.H. Robinson, S. Richardson, S.W. Evans, R. Stallworth, and M. Hovater, "Foam-on-tile Impact Modeling for the STS-107 Investigation," AIAA-2004-0938, presented at the 2004 AIAA Aerospace Sciences Meeting, Reno, Nevada, January 5-8,2004.

4. J.M. McGlaun, S.L. Thompson, and M.G. Elrick, 1990, "CTH: A three dimensional shock wave physics code," International Journal of Impact Engineering, Volume 10, pp. 351-360.

5. K.W. Gwinn and K.E. Metzinger, "Analysis of Foam Impact Onto the Columbia Shuttle Wing Leading Edge Panels Using Pronto3D/SPH," AIAA-2004-0942, presented at the 2004 AIAA Aerospace Sciences Meeting, Reno, Nevada, January 5-8,2004.

6. Fahrenthold, E.P., and Horban, B.A., 2001, "An improved hybrid particle-finite element method for hypervelocity impact simulation," International Journal of Impact Engineering, Vol. 26, pp. 169-178.

7. Fahrenthold, E.P., User's Guide for EXOS, University of Texas, Austin, Texas, 2003.

8. Shivarama, R., and Fahrenthold, E.P., 2004, "An ellipsoidal particle-finite element method for hypervelocity impact simulation," International Journal for Numerical Methods in Engineering, Volume 59, pp. 737-753.

9. Fahrenthold, E.P., and Shivarama, R., 2003, "Extension and validation of a hybrid particle-finite element method for hypervelocity impact simulation," International Journal of Impact Engineering, Volume 29, pp. 237-246.

10. L.E. Malvern, 1969, Introduction to the Mechanics of a Continuous Medium, Prentice Hall, Englewood Cliffs, New Jersey.

11. M. Melis, K. Carney, M. Pereira, D. Revilock, and P. Kopfinger, "Characterization of BX-250 ET Foam Behavior Under Impact in a 1 psi Environment," AIAA-2004-0943, oral presentation at the 2004 AIAA

Aerospace Sciences Meeting, Reno, Nevada, January 5-8,2004.

12. W.-Y. Lu, B.R. Antoun, J.S. Korellis, S. Scheffel, M.Y. Lee, R.D. Hardy, and L.S. Costin, "Material Characterization of Shuttle Thermal Protection System for Impact Analyses," AIAA-2004-0945, presented at the 2004 AIAA Aerospace Sciences Meeting, Reno, Nevada, January 5-8,2004.

13. J.W. Sawyer, "Mechanical Properties of the Shuttle Orbiter Thermal Protection System Strain Isolator Pad," AIAA-1982-0789.

14. P.A. Cooper and J.W. Sawyer, 1983, "Life Considerations of the Shuttle Orbiter Densified-Tile," in Shuttle Performance: Lessons Learned, NASA Conference Publication 2283, pp. 1009-1024.

15. Oertel, G., editor, 1994, Polyurethane Handbook, Hanser/Gardner, New York.

16. R.P. Banas, D.E. Elgin, E.R. Cordia, K.N. Nickel, E.R. Gzowski, and L. Aguilar, 1983, "Lessons Learned from the Development and Manufacturing of Ceramic Reusable Surface Insulation Materials for the Space Shuttle Orbiters," in Shuttle Performance: Lessons Learned, NASA Conference Publication 2283, pp. 967-1008.

17. D.E. Myers, C.J. Martin, and M.L. Blosser, 2000, "Parametric Weight Comparison of Advanced Metallic, Ceramic Tile, and Ceramic Blanket Thermal Protection Systems," NASA TM 2000-210289.

18. C.W. Ohlhorst, W.J. Vaughn, P.O. Ransone, and H.T. Tsou, 1997, "Thermal Conductivity Database of Various Structural Carbon-Carbon Composite Materials," NASA TM 1997-4787.

19. DuPont Corporation, 2001, Technical Guide for Nomex Brand Fiber, H-52720.

Table 1. Material properties

| *Material property* | *Foam* | *Tile* | *SIP* | *RCC* |
|---|---|---|---|---|
| Young's modulus (psi) | 1,360 | 9,022 | 220 | $2.21\times10^{6}$ |
| Shear modulus (psi) | 529 | 3,510 | 110 | $1.04\times10^{6}$ |
| Reference density ($lb/ft^3$) | 2.15 | 9.00 | 12.3 | 98.6 |
| Yield stress (psi) | 42.2 | 23.9 | 27.4 | $14.0\times10^{3}$ |
| Specific heat (Btu/lbm-degree F) | 0.454 | 0.151 | 0.315 | 0.171 |
| Thermal expansion coefficient (1/degree F) | 0 | $2.25\times10^{-7}$ | $1.00\times10^{-5}$ | $7.28\times10^{-7}$ |
| Plastic failure strain | 1.0 | 1.0 | 1.0 | 0.01 |

Table 2. Parameters of the tile impact simulations

| *Parameter* | *MLGD 1* | *MLGD 2* | *MLGD 3* | *Wing Acreage* |
|---|---|---|---|---|
| Projectile velocity (fps) | 700 | 700 | 700 | 720 |
| Impact obliquity (degrees) | 5 | 5 | 5 | 13 |
| Projectile roll (degrees) | 90 | 0 | 0 | 0 |
| Projectile cross section (in) | 3.5×11.5 | 3.5×11.5 | 5.5×11.5 | 5.5×11.5 |
| Projectile length (in) | 21.25 | 21.25 | 28.5 | 19.0 |
| Tile thickness (in) | 1.875 | 1.875 | 1.700 | 2.450 |
| Aluminum plate thickness (in) | 0.1875 | 0.1875 | 0.2689 | 0.2720 |
| Simulation time (milliseconds) | 5.0 | 5.0 | 6.0 | 5.0 |
| Number of particles (millions) | 1.10 | 1.10 | 1.42 | 1.48 |
| Number of processors (SGI Origin) | 128 | 128 | 192 | 192 |
| Wall clock time (hours) | 76.5 | 90.1 | 127 | 102 |

Table 3. Parameters of the wing leading edge impact simulations

| *Parameter* | *Corner impact case* | *Edge impact case* |
|---|---|---|
| Projectile velocity (fps) | 775 | 775 |
| Projectile dimensions (in) | 5.5×11.5×22.8 | 5.5×11.5×22.8 |
| Projectile roll, pitch, yaw (degrees) | 0.0, 17.5, 6.32 | 30.0, 17.5, 6.32 |
| Impact obliquity (degrees) | 14.6 | 14.6 |
| Panel dimensions (in) | 20.5×38.4×21.3 | 20.5×38.4×21.3 |
| Panel thickness (in) | 0.25 | 0.25 |
| Simulation time (milliseconds) | 1.635 | 2.000 |
| Number of particles (millions) | 1.90 | 1.90 |
| Number of processors (SGI Origin) | 128 | 256 |
| Wall clock time (hours) | 96 | 74 |

Figure 1. Simulation results for case MLGD 1.

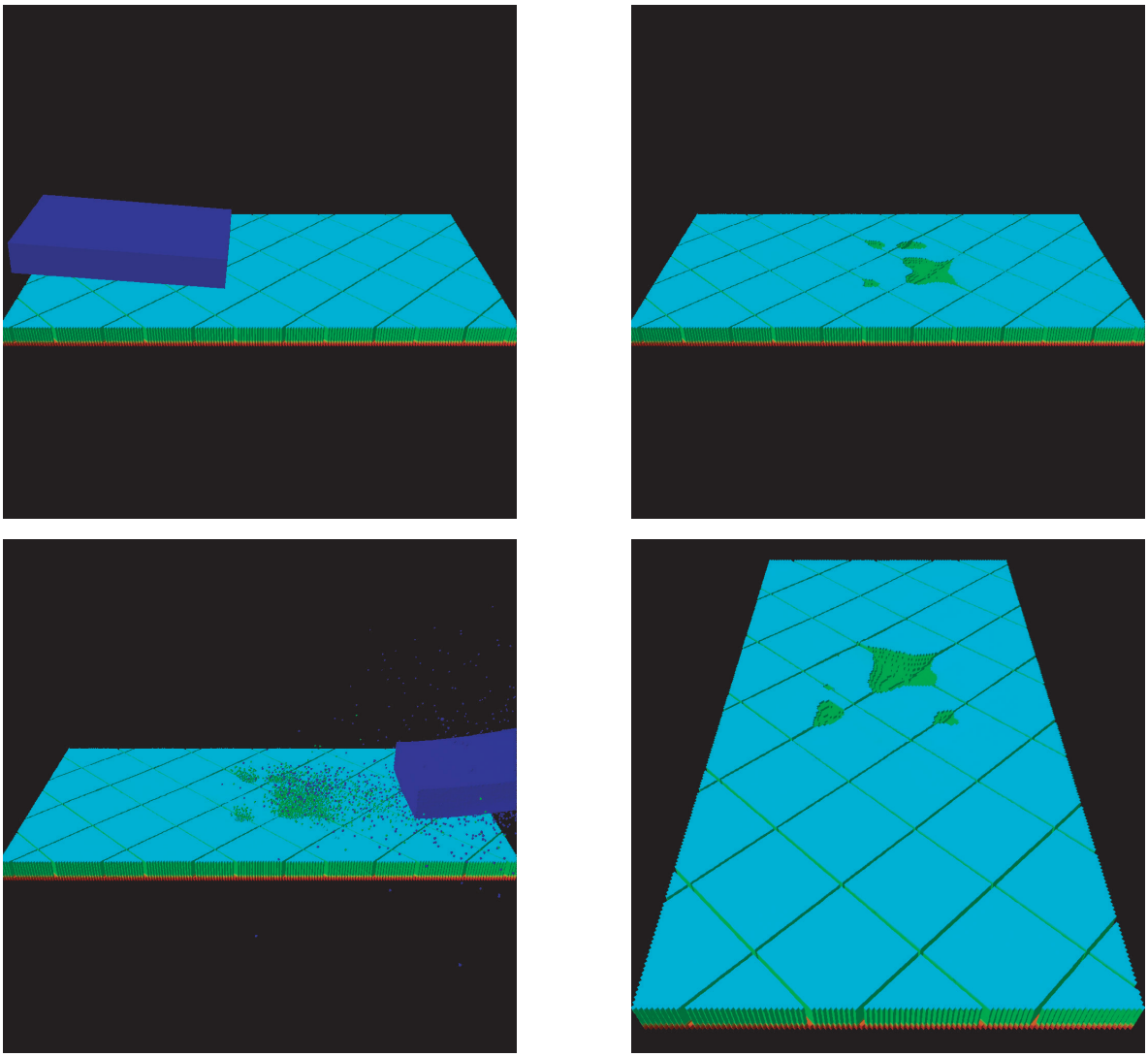

Figure 2. Simulation results for case MLGD 2.

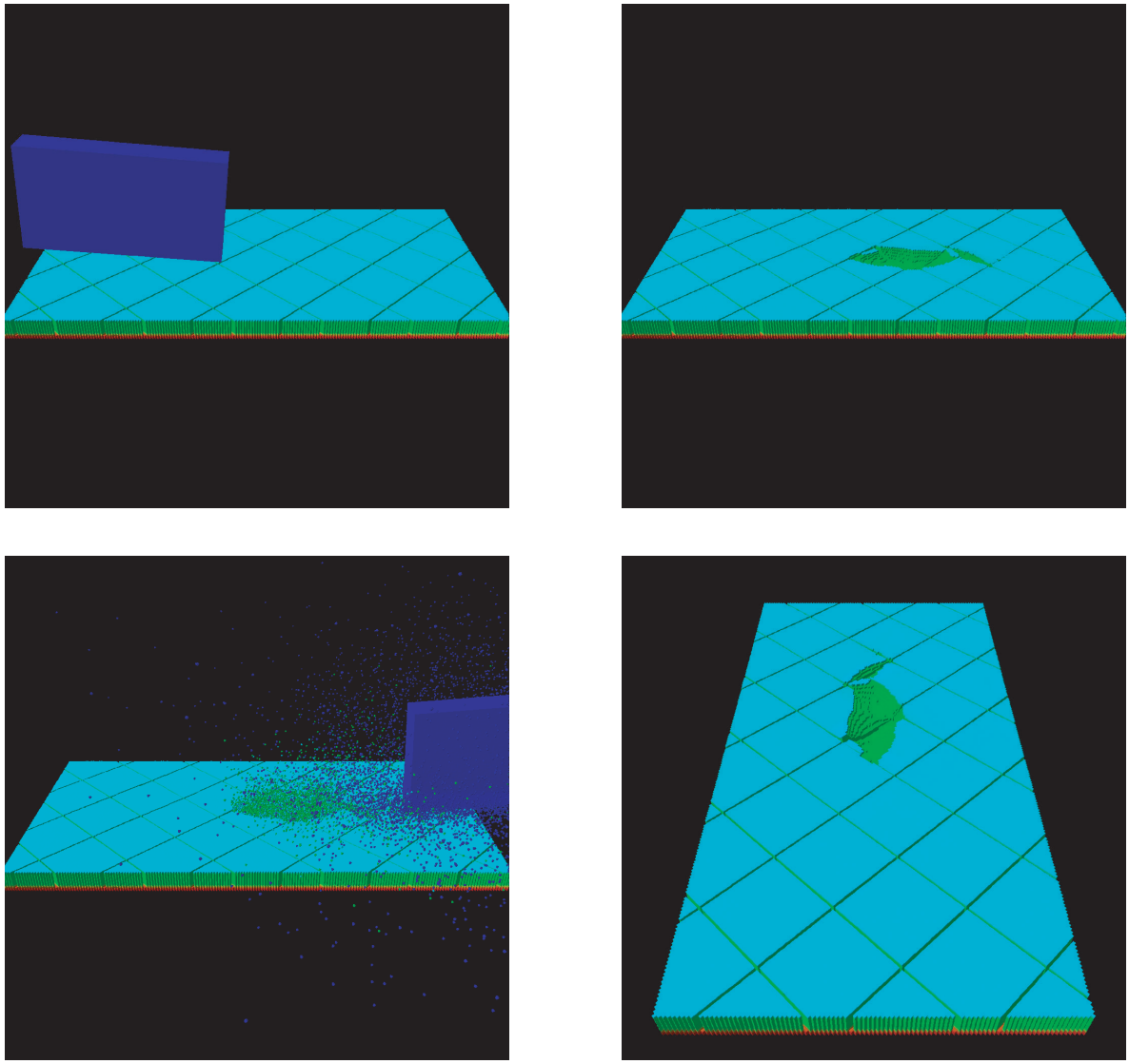

Figure 3. Simulation results for case MLGD 3.

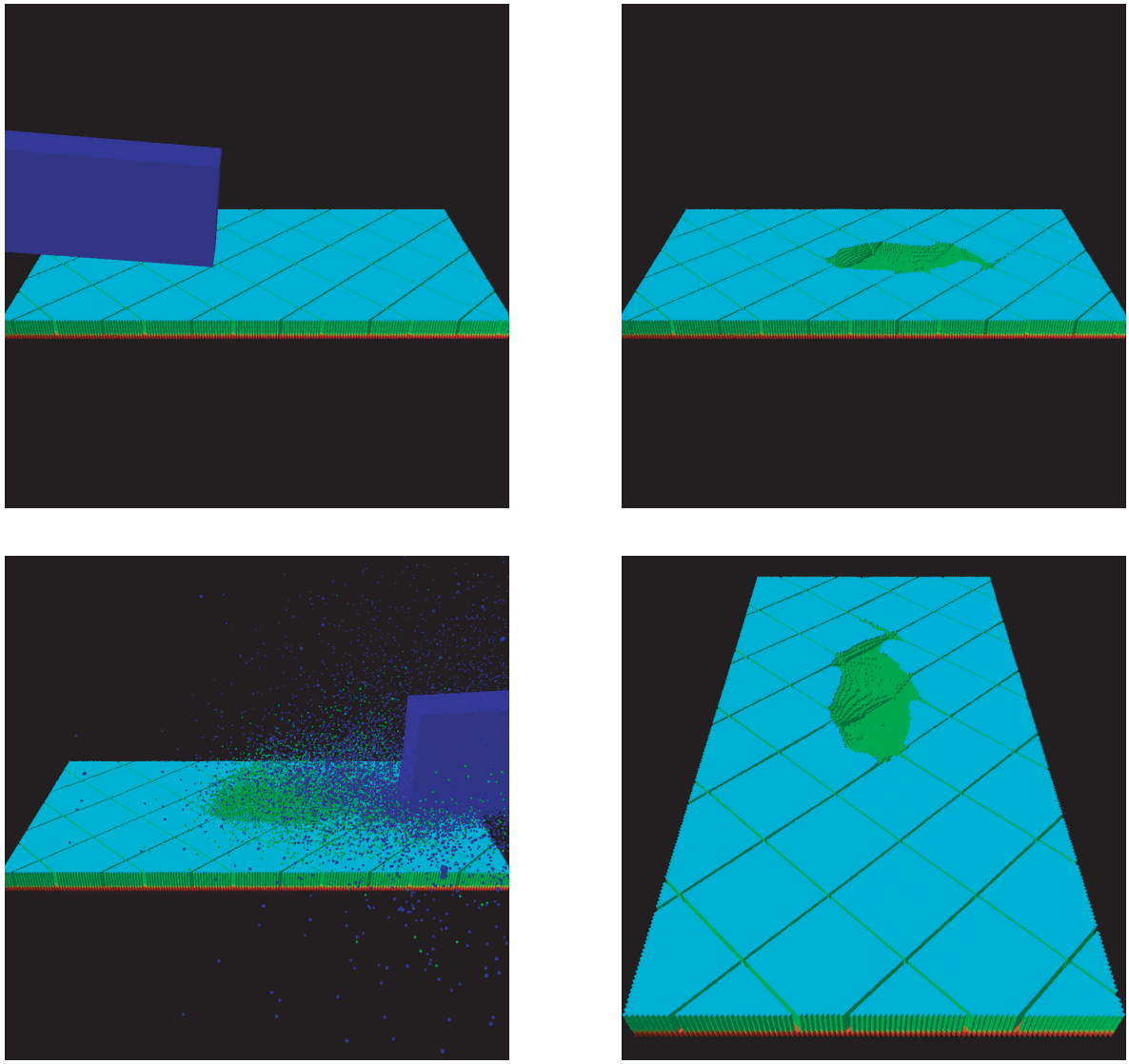

Figure 4. Simulation results for the wing acreage impact case.

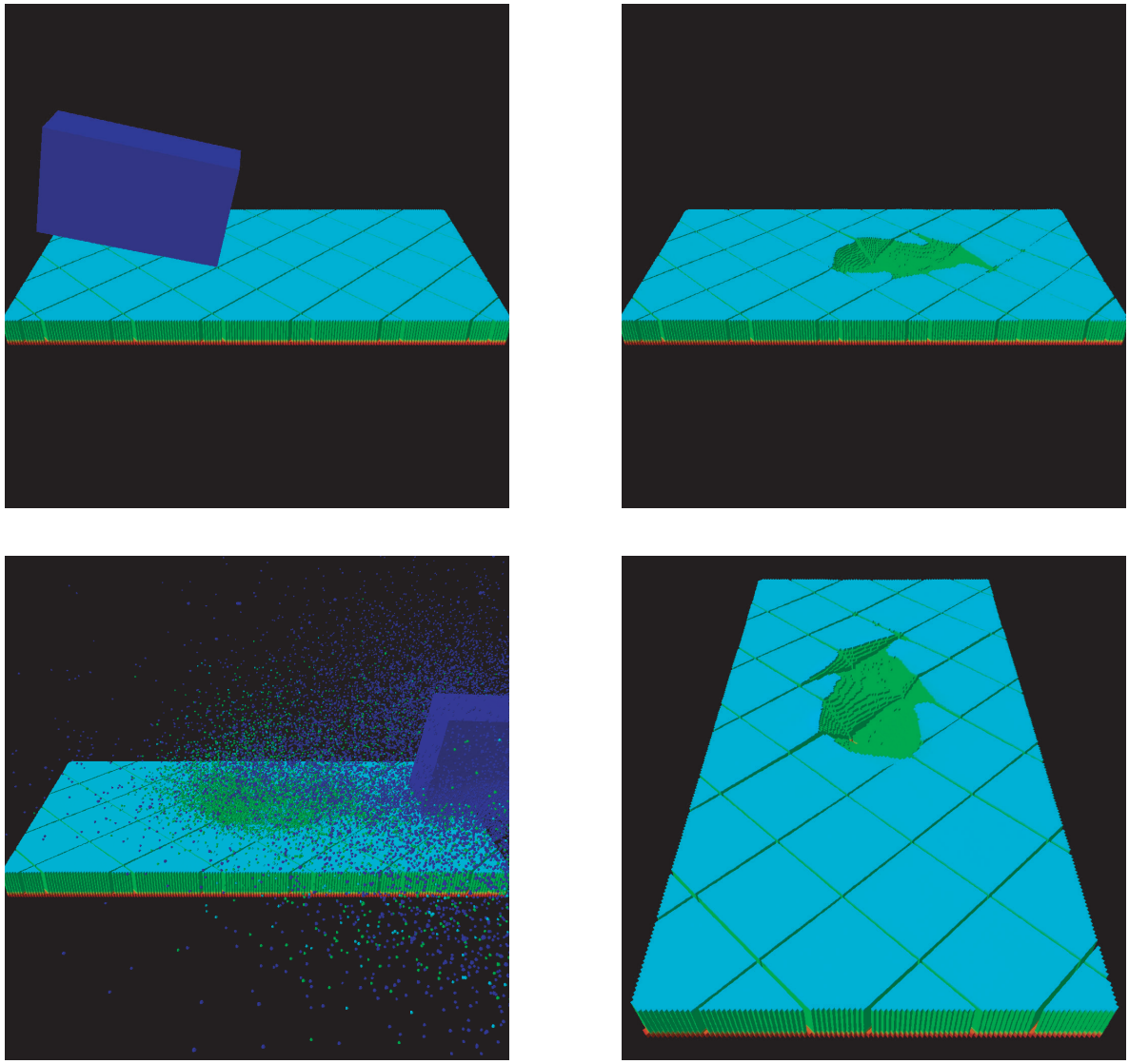

Figure 5. Simulation results for the RCC corner impact case.

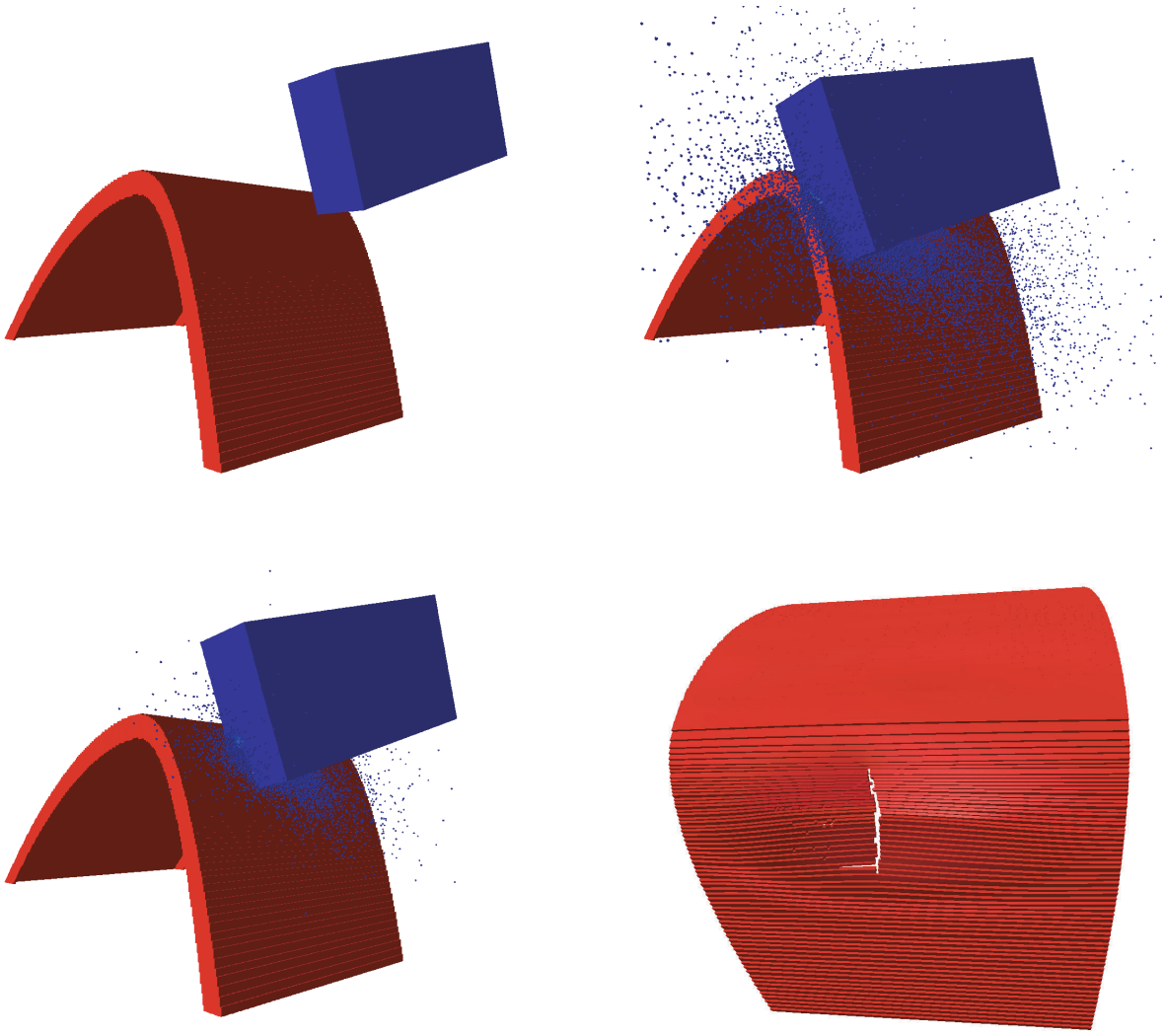

Figure 6. Simulation results for the RCC edge impact case.

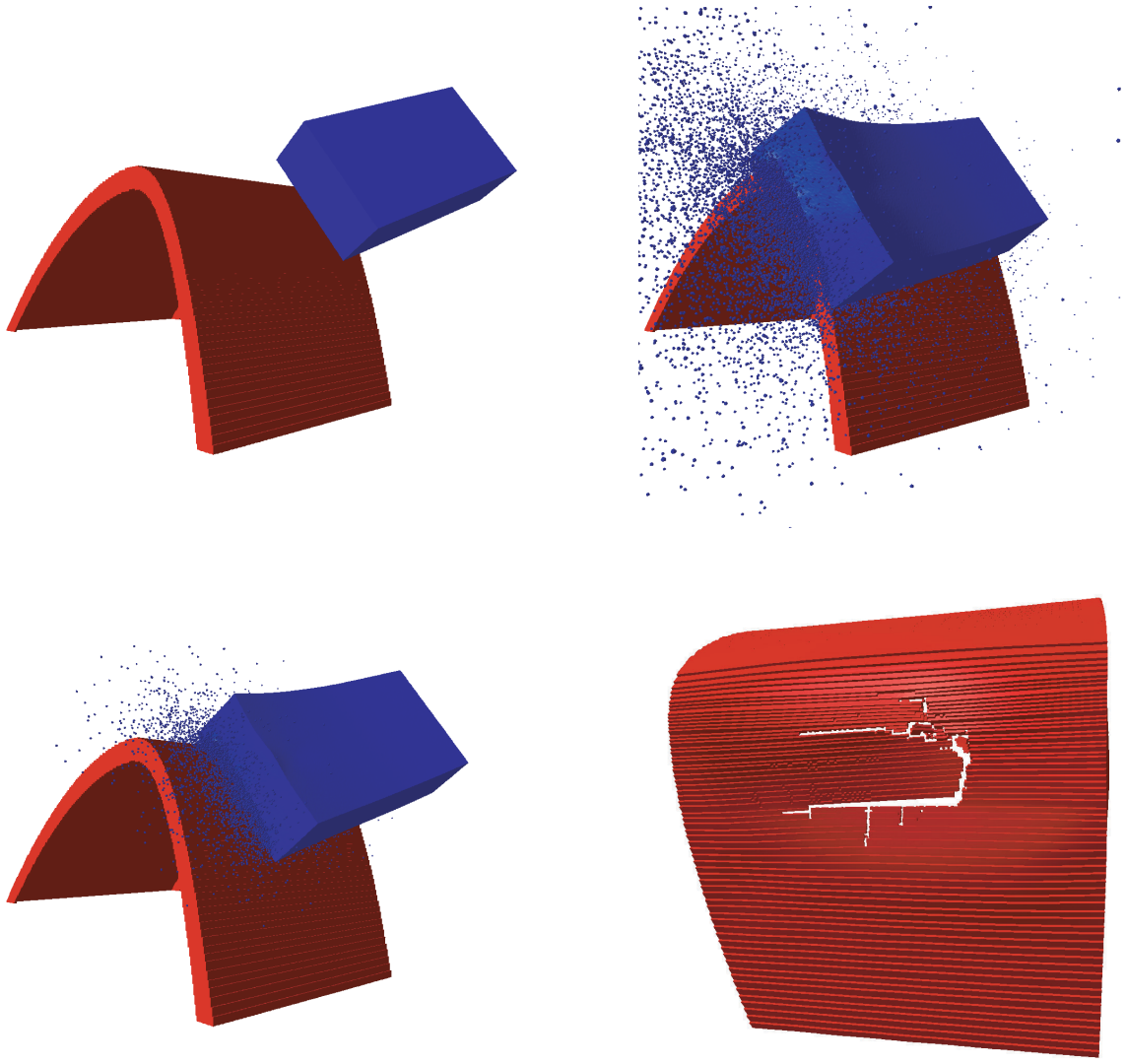

# CONCLUSIONS

The design of manned spacecraft for future space exploration missions will require consideration of micrometeoroid and orbital debris impact effects. The debris environment in low earth orbit presents a significant hazard, and has mandated the development of hypervelocity impact shielding for the International Space Station. Although exposure times for the Space Shuttle are much less than that for the space station, the shuttle routinely suffers limited orbital debris impact damage. Hence next generation spacecraft intended to operate, even for limited periods, in low earth orbit must be designed with the orbital debris impact threat in mind. For operations beyond earth orbit, the principal impact threat is due to micrometeoroids. Micrometeoroid impacts typically involve lower particle masses and densities, but higher impact velocities, than those associated with man-made debris in low earth orbit. As a result, shielding designed for low earth orbit projectiles may not be optimal to address the significant micrometeoroid hazard. Although considerable previous work has focused on the hypervelocity impact shielding problem, the development of next generation spacecraft is likely to require significant new experimental and computational research efforts. There are two principal reasons. The first is that the current knowledge base is focused heavily on projectiles, shielding, and spacecraft structures composed of metals. The second is that current experimental methods are not able to address the full impact velocity and kinetic energy range of interest. Although previous experimental and computational studies of debris shielding have involved composites, work to date has served to highlight the increased complexity and cost of experimental and computational impact work involving advanced materials. The research described here on hypervelocity impact effects in reinforced carbon-carbon illustrates a design methodology likely to apply in future development of manned vehicles for space exploration missions. Coordinated experimental and computational efforts will likely be required to address orbital debris and micrometeoroid related design requirements for new space exploration systems.

# APPENDIX 1

## Simulation Data for Reinforced Carbon-Carbon

| Simulation number | $D$ (cm) | $v$ (km/s) | $\phi$ (deg) | $N_e$ | Equation of state | $D_p$ (cm) | Error (%) | $D_c$ (cm) | Error (%) |
|---|---|---|---|---|---|---|---|---|---|
| 200 | 0.628 | 7.01 | 45 | 8 | Mie Gruneisen | 2.60 | 10.3 | 3.74 | 15.0 |
| 219 | | | | 8 | SESAME 3715 | 2.65 | 8.6 | 3.60 | 18.2 |
| 211 | | | | 16 | Mie Gruneisen | 2.66 | 8.3 | 4.05 | 8.0 |
| 218 | | | | 24 | Mie Gruneisen | 2.67 | 7.9 | 4.08 | 7.3 |
| 201 | 0.478 | 6.96 | 30 | 8 | Mie Gruneisen | 2.12 | 3.6 | 2.95 | 21.3 |
| 220 | | | | 8 | SESAME 3715 | 1.97 | 10.5 | 2.95 | 21.3 |
| 212 | | | | 16 | Mie Gruneisen | 2.00 | 10.0 | 3.38 | 9.9 |
| 221 | | | | 24 | Mie Gruneisen | 2.10 | 4.5 | 3.48 | 7.2 |
| 191 | 0.123 | 7 | 30 | 8 | Mie Gruneisen | 0.159 | na | nr | na |
| 192 | | 10 | | 8 | Mie Gruneisen | 0.390 | na | nr | na |
| 193 | | 13 | | 8 | Mie Gruneisen | 0.536 | na | nr | na |
| 188 | 0.240 | 7 | 30 | 8 | Mie Gruneisen | 0.95 | na | nr | na |
| 189 | | 10 | | 8 | Mie Gruneisen | 1.21 | na | nr | na |
| 190 | | 13 | | 8 | Mie Gruneisen | 1.54 | na | nr | na |
| 185 | 0.360 | 7 | 30 | 8 | Mie Gruneisen | 1.41 | na | nr | na |
| 186 | | 10 | | 8 | Mie Gruneisen | 1.84 | na | nr | na |
| 187 | | 13 | | 8 | Mie Gruneisen | 2.22 | na | nr | na |
| 224 | 0.360 | 7 | 30 | 8 | SESAME 3715 | 1.50 | na | 2.00 | na |
| 223 | | 10 | | 8 | SESAME 3715 | 1.83 | na | 2.75 | na |
| 222 | | 13 | | 8 | SESAME 3715 | 2.33 | na | 3.17 | na |

na = not available (no corresponding experiment)

nr = not recorded (accurate coating spall results require $N_e = 16$)

$D$ = projectile diameter (aluminum sphere)

$v$ = impact velocity; $\phi$ = impact obliquity (normal impact is zero degrees)

$N_e$ = number of elements across the target plate

$D_p$ = perforation diameter; $D_c$ = diameter of the spalled coating region